HHS Public Access

Author manuscript

Nat Med. Author manuscript; available in PMC 2017 May 21.

Published in final edited form as:

Nat Med. 2017 January ; 23(1): 120–127. doi:10.1038/nm.4232.

Systemic depletion of serum L-Cyst(e)ine with an engineered human enzyme induces production of reactive oxygen species and suppresses tumor growth in mice

Shira L. Cramer[1,π], **Achinto Saha**[2,π], **Jinyun Liu**[3,π], **Surendar Tadi**[4], **Stefano Tiziani**[4], **Wupeng Yan**[5], **Kendra Triplett**[1,5], **Candice Lamb**[1,5], **Susan E. Alters**[6], **Scott Rowlinson**[6], **Yan Jessie Zhang**[5], **Michael J. Keating**[7], **Peng Huang**[3], **John DiGiovanni**[2], **George Georgiou**[1,5,*], and **Everett Stone**[5,*]

[1]Department of Chemical Engineering, The University of Texas at Austin, Austin, TX 78712, United States

[2]Division of Pharmacology and Toxicology and Dell Pediatric Research Institute, The University of Texas at Austin, Austin, TX 78712, United States

[3]Department of Translational Molecular Pathology, The University of Texas MD Anderson Cancer Center, Houston, TX 77030, United States

[4]Department of Nutritional Sciences, The University of Texas at Austin, Austin, TX 78712, United States

[5]Department of Molecular Biosciences, The University of Texas at Austin, Austin, TX 78712, United States

[6]Aeglea Biotherapeutics, Austin, TX 78746, United States

[7]Department of Leukemia, The University of Texas MD Anderson Cancer Center, Houston, TX 77030, United States

Abstract

Cancer cells experience higher oxidative stress from reactive oxygen species (ROS) than non-malignant cells due to genetic alterations and abnormal growth and as a result, maintenance of the anti-oxidant glutathione (GSH) is essential for their survival and proliferation[1–3]. Under elevated

*Correspondence to: gg@che.utexas.edu (G.G.); stonesci@utexas.edu (E.S.).
πEqual contribution.

Accession codes: The Cyst(e)inase structure has deposited into the Worldwide Protein Data Bank with the PDB code of 5EIG.

Data Availability Statement: Data collection and refinement statistics for the Cyst(e)inase structure (PDB:5EIG) are summarized in Supplementary Table 1.

Author Contributions: S.L.C., A.S., J.L., S. Tadi., W.Y., K.T., C.L., and Y.J.Z. performed key experiments; E.S., P.H., J.D. and G.G. conceived and designed the research; S.L.C., A.S., J.L., S. Tadi., S. Tiziani, W.Y., K.T., S.E.A., S.R., Y.J.Z., M.J.K, P.H., J.D., G.G., and E.S. analyzed data; M.J.K. provided critical materials (CLL blood samples); S.L.C., A.S., J.L., G.G., J.D. and E.S. wrote the manuscript.

Competing Financial Interests Statement: G. Georgiou, and E. Stone are inventors on intellectual property related to this work and G. Georgiou, E. Stone, S. Rowlinson and S. Alters have an equity interest in Aeglea Biotherapeutics, a company pursuing the commercial development of this technology.

ROS conditions endogenous L-Cysteine (L-Cys) production is insufficient for GSH synthesis, necessitating L-Cys uptake, predominantly in its disulfide form L-Cystine (CSSC) via the xCT(−) transporter. Here we show that administration of an engineered, pharmacologically optimized, human Cyst(e)inase enzyme mediates sustained depletion of the extracellular L-Cys and CSSC pool in mice and non-human primates, selectively causes cell cycle arrest and death (PI and Annexin-V staining) in cancer cells due to depletion of intracellular GSH and ensuing elevated ROS, yet results in no apparent toxicities in mice even after months of continuous treatment. Cyst(e)inase suppressed the growth of prostate carcinoma allografts, reduced tumor growth in prostate and breast cancer xenografts and doubled the median survival time of *TCL1*-Tg:*p53*$^{-/-}$ mice that develop disease resembling human chronic lymphocytic leukemia. The observation that enzyme-mediated depletion of the serum L-Cys and CSSC pool suppresses the growth of multiple tumors, yet is very well tolerated for prolonged periods suggests that Cyst(e)inase represents a safe and effective therapeutic modality for inactivating anti-oxidant cellular responses in a wide range of malignancies[4,5].

As a precursor for the biosynthesis of GSH, L-Cys is essential for maintaining the intracellular thiol redox potential. L-Cys is produced via the transsulfuration pathway enzymes cystathionine-β-synthase (CBS) and cystathionine-γ-lyase (CGL), which are widely expressed in numerous tissues in humans (Fig. 1a)[6–9]. In contrast, some tumors have markedly lower expression of transsulfuration enzymes namely due to transcriptional silencing[10,11], or endogenous L-Cys synthesis is insufficient because rapid proliferation, metabolic dysregulation, and oncogene expression markedly increase ROS levels. Consequently, import of extracellular L-Cys becomes necessary to meet cellular GSH requirements[12–16]. The main route for extracellular acquisition of L-Cys is transport of its disulfide form, CSSC, through the xCT(−) CSSC/L-glutamate (L-Glu) antiporter (SLC7A11) (Fig. 1a). Due to high demand for CSSC in numerous malignancies, xCT(−) represents a key therapeutic target with small molecule inhibitors of the transporter displaying anti-tumor effects[12–15]. As L-Cys is a non-essential amino acid in animals, eliminating L-Cys and CSSC uptake should selectively impact tumors displaying increased ROS production and thus a higher demand for anti-oxidants, without adversely affecting normal physiology. However, inhibition of xCT(−) alone is insufficient because free L-Cys is imported via other transporters (e.g. the system ASC transporters ASCT1 and ASCT2). Instead, a superior approach to small molecule inhibition of multiple transporters is to eliminate the extracellular pool of L-Cys and CSSC through the action of an enzyme that converts these amino acids into non-toxic, readily metabolizable, products.

The pyridoxal phosphate (PLP)-dependent enzyme CGL (EC 4.4.1.1) catalyzes the last step in *de novo* L-Cys synthesis, converting L-cystathionine (L-Cysta) into α-ketobutyrate, L-Cys, and NH_4^+. CGL can also accept L-Cys or CSSC as substrates producing pyruvate, NH_4^+, and H_2S or thiocysteine respectively. Although CGL can degrade both CSSC and L-Cys, its kinetics are too slow to be relevant for clinical applications given that dosing at >2 g/kg would be required to achieve substantial reduction of serum L-Cys and CSSC levels in mice. Structural analyses of CGL (PDB:3COG) suggested that amino acid substitutions of active site residues E59 and E339, which are important for L-Cysta coordination, could enhance L-Cys and CSSC degrading activity. Combinatorial saturation mutagenesis of these residues

coupled with a high throughput assay for pyruvate production led to the isolation of CGL-E59T-E339V, displaying 50- and 25-fold higher k_{cat}/K_M values for CSSC and L-Cys respectively, than WT-CGL (Fig. 1b). Solving the X-ray structure of CGL-E59T-E339V in the presence of 1 mM L-Cys at 2.7Å revealed an essentially identical structure to WT-CGL with only minor perturbations at the mutation sites (0.66 Å RMS to PDB:2NMP); as well as substrate complexes within the four active sites of the tetramer (Supplementary Table 1). In two active sites, the amine of the substrate L-Cys forms a geminal diamine with the PLP cofactor and the ε-amine of Lys212, representing a reaction intermediate just prior to forming the L-Cys-external aldimine complex, which is further stabilized by a salt bridge to the L-Cys α-carboxyl group and the guanidinium moiety of Arg375 (Fig. 1c). Collectively, the structural and kinetic data indicate that the E339V substitution increases the hydrophobicity of the active-site to enhance L-Cys binding[17,18] while the removal of the E339 and E59 carboxyl groups better accommodates CSSC binding, a conclusion that is further supported by molecular dynamic modeling (Supplementary Fig. 1).

To prevent renal clearance and thus impart long circulation persistence, CGL-E59T-E339V was conjugated to methoxy PEG succinimidyl carboxymethyl ester, MW 5000 Da (Supplementary Fig. 2) (conjugated protein henceforth referred to as Cyst(e)inase). Single dose administration of Cyst(e)inase at 8 mg/kg to two cynomolgus monkeys resulted in a marked reduction in total serum L-Cys content (Free+liberated protein-bound L-Cys and CSSC) for 28 hours (Fig. 1d) with no observed toxicities (based on hematology, blood chemistry and animal observations, see Supplementary Data Set 1), indicating that Cyst(e)inase is able to modulate blood L-Cys and CSSC levels in primates.

Increased ROS production has been widely noted in human prostate carcinomas (PCa) with high levels correlating with an aggressive phenotype[19–21]. We therefore evaluated the effect of Cyst(e)inase on the human PCa cell lines PC3 and DU145; as well as the murine PCa cell line, HMVP2[22] derived from the ventral prostate of HiMyc transgenic mice[23]. The HMVP2 murine PCa cell line constitutes a relevant model to human disease as it possesses characteristics of cancer stem cells, expresses stem cell markers (such as LIN^{neg}, Sca-1^{high}, $CD49f^{high}$, CK14, and CD29), and produces spheroids[22]. Cyst(e)inase potently inhibited survival of HMVP2 cells with an IC_{50} of 23 ± 4 nM (Fig. 2a). A dose-dependent significant increase in ROS ($P<0.001$) was evident by 4 hours after enzyme addition, with a concomitant significant ($P< 0.001$) decrease in cellular GSH levels by 24 hours (Fig. 2b,c). Consistent with the well-established effects of ROS accumulation and amino acid restriction in eliciting autophagic responses[24–26], Cyst(e)inase treatment increased AMPK phosphorylation ($pAMPK^{Thr172}$) (Fig. 2d), reduced phosphorylated mTOR ($pmTOR^{Ser2448}$), and increased autophagic responses manifested by changes in the phosphorylation levels of mTORC1 and downstream genes such as p70S6K, ribosomal protein S6 and ULK1 as well as LC-3 II formation (Fig. 2e,f). Similarly, Cyst(e)inase treatment of the human cell line PC3 resulted in dose-dependent cell killing, a 4–6–fold increase of $pAMPK^{Thr172}$ and increased autophagic responses (Supplementary Fig. 3a–d). AMPK and p70S6K can also directly affect cell cycle progression[27,28], and we observed a significant dose-dependent arrest in G_0/G_1 with a corresponding significant decrease of cells in S-phase and a non-significant but slight increase in G_2/M populations (Fig. 2g). The G_0/G_1 arrest was accompanied with a dose-dependent increase in protein levels of the cyclin-dependent kinase

inhibitor p27 (> 7-fold, Fig. 2h), whose accumulation can be stabilized by pAMPK[27]. We also detected decreased protein levels of c-Myc, the cyclin-dependent kinases CDK2 and CDK4, phosphorylated retinoblastoma protein (pRB$^{Ser807/811}$), E2F4, and cyclins A, D1 & E1 (Fig. 2h,i). Conversely, and consistent with a ROS driven mechanism, we found that treating cells with the ROS scavenger and L-Cys donor *N*-acetyl-L-cysteine, partially restored survival (Fig. 2j and Supplementary Fig. 3e).

To assess Cyst(e)inase anti-tumor activity *in vivo* in murine models, we first established an appropriate dosing schedule by measuring the pharmacokinetics of Cyst(e)inase and its pharmacodynamics effect on thiol-containing metabolites in serum in mice. Following single dose i.p. (50 mg/kg) administration of Cyst(e)inase in non-tumor bearing FVB mice, we observed a clearance half-life of 25 ± 2 hrs with the data fitting well to an extravascular clearance model[29] (Fig. 3a). Similar to the observations in cynomolgus monkeys, no weight loss, adverse effects, nor organ abnormalities upon necropsy were observed in the mice (data not shown). Time course serum metabolomics analyses revealed near complete elimination of serum CSSC for 4 days, before recovering to pre-administration concentrations at day 6 (Fig. 3b). Free L-Cys levels were reduced by over 4-fold for 2 days before gradually recovering (Fig. 3b). The impact of Cyst(e)inase on the concentration of other sulfur containing metabolites was consistent with their respective steady-state serum concentrations, enzyme kinetics, and the consequences of depleting extracellular L-Cys and CSSC (Supplementary Fig. 4). From a clinical translation standpoint this treatment corresponds to realistic clinical doses (based on allometric scaling, a 50 mg/kg dose in mice corresponds 6.5 mg/kg in humans[30]).

We then treated (via i.p. injection) syngeneic male FVB/N mice bearing palpable HMVP2 tumors with either 50 or 100 mg/kg Cyst(e)inase, and PBS or 100 mg/kg heat-inactivated Cyst(e)inase as controls every 4 days for 4 weeks. Tumors did not increase in size in either Cyst(e)inase-treated group, while mice injected with heat-inactivated enzyme (a control for the presence of residual impurities and endotoxin in active protein) showed identical tumor growth to the PBS-treated group (Fig. 3c). Throughout the treatment period, no weight loss or inappetence was observed (Fig. 3d), nor were any adverse effects as determined by examination of tissues upon necropsy (data not shown).

Similarly, Cyst(e)inase treatment in male nude mice under the same dosing schedule significantly blocked growth of both DU145 ($P<0.0001$ at 100 mg/kg, Fig. 3e) and PC3 xenograft tumors ($P<0.0001$ at 50 and 100 mg/kg; Fig. 3f). Once again no weight loss or inappetance was observed, nor were changes in blood cell counts or blood chemistry (Supplementary Figs. 5, 6). Macroscopically (at the time of sacrifice), the liver and other major organs in treated mice looked similar to control with no obvious signs of toxicity (data not shown). We also examined H&E stained sections of liver tissue from both control and treated mice microscopically. The liver of Cyst(e)inase treated mice was normal in histologic appearance, maintaining normal hepatic architecture with no obvious signs of cellular toxicity (data not shown). Because ocular tissues are known to have a high demand for CSSC[31,32], we also performed histological examinations of ocular sections and found no evidence of changes in tissue ultrastructure compared to control groups, further underscoring that Cyst(e)inase treatment is well tolerated (data not shown). In addition to prostate

carcinomas, Cyst(e)inase may be beneficial for the treatment of a wide range of cancers, notably human breast carcinomas, which upregulate xCT(−)[12,33]. Accordingly, Cyst(e)inase administration significantly abrogated the growth of MDA-MB-361 breast cancer xenografts orthotopically implanted into female NOD SCID mice ($P<0.0001$ at 50 and 100 mg/kg; Supplementary Fig. 7), suggestive of a common tumoral dependence on L-Cys and CSSC.

To further confirm Cyst(e)inase impacts tumors by affecting cellular thiol anti-oxidant pathways, we investigated the effect of Cyst(e)inase in combination with well-established drug candidates targeting the GSH or thioredoxin (TXN)- thioredoxin reductase (TXNR) pathways. For these studies we used respectively, buthionine sulfoximine (BSO) which inhibits GSH synthesis, and the natural product curcumin (which is the active component of turmeric) that irreversibly inhibits TXNR[34], and is being evaluated in numerous clinical trials as a therapy for various neoplasias[35–37]. We compared the effects of Cyst(e)inase with BSO or curcumin alone, and in combination on DU145 PCa cell viability using an MTT assay. Cyst(e)inase was far more cytotoxic than BSO alone, but the combination showed a synergistic effect (Supplementary Fig. 8a). Similarly, we observed that curcumin synergized with Cyst(e)inase in DU145 cells and in the very aggressive, castrate resistant PCa cell line 22Rv1 (Supplementary Fig. 8b,c). Cyst(e)inase treatment in combination with either BSO or curcumin led to a significant increase in cellular ROS levels ($P<0.01$ as compared to treatment with individual agents) (Supplementary Fig. 8d–f). *In vivo*, and consistent with the *in vitro* results, only slight tumor inhibition was observed in male nude mice implanted with 22Rv1 cells when treated with moderate Cyst(e)inase (25 mg/kg) or curcumin (1% w/w in diet) doses, whereas co-administration of Cyst(e)inase and curcumin significantly enhanced tumor growth inhibition (Supplementary Fig. 8g). Notably, treatment with a higher dose of Cyst(e)inase (100 mg/kg) as a single agent displayed analogous efficacy to the combination treatment (Supplementary Fig. 8g), suggesting that Cyst(e)inase-treatment simultaneously effects both the GSH and TXN anti-oxidant pathways.

Recently Huang *et al.* reported that primary leukemia cells isolated from chronic lymphocytic leukemia (CLL) patients rely on cysteine uptake for GSH production, but have low xCT(−) expression[16]. Consequently, CLL cell viability is dependent on stromal protection, where surrounding bone marrow stromal cells (which highly express xCT(−)) uptake CSSC for conversion to L-Cys, which is then released into the microenvironment for uptake by CLL cells (via system ASC transporters). The reliance of CLL cells on stromal protection is further shown *in vitro*, where a high level of spontaneous apoptosis is observed in CLL cells cultured alone, yet co-culture with stromal cells significantly enhances cell viability[16]. Accordingly, we compared the effect of Cyst(e)inase to the CLL standard of care drug fludarabine (or their combination) in mouse leukemic cells isolated from *TCL1*-Tg:$p53^{-/-}$ mice, a model with a *TCL1* transgenic and *p53* deletion genotype that exhibits highly aggressive disease progression with 100% penetrance and a drug resistant phenotype that mimics human CLL with a chromosomal 17p deletion (which is associated with poor clinical outcomes)[38]. *TCL1*-Tg:$p53^{-/-}$ mice develop splenomegaly, with IgM+CD5+ B leukemic cells representing 80–90% of total cells in the spleen. *TCL1*-Tg:$p53^{-/-}$ splenocytes co-cultured with murine stromal Kusa-H cells (to mimic the protective CLL microenvironment) were minimally affected by fludarabine, yet were potently killed by Cyst(e)inase (Fig. 4a and Supplementary Fig. 9).

We then performed a long-term survival experiment in *TCL1*-Tg:$p53^{-/-}$ mice treated with either fludarabine, Cyst(e)inase, or their combination starting at ~ 2 months of age, at which point the mice begin to develop disease. As shown in Fig. 4b, untreated *TCL1*-Tg:$p53^{-/-}$ mice (n = 47) displayed a median survival time of 3.5 months whereas fludarabine treatment improved the median survival time to 5.3 months ($p < 0.001$). Consistent with the *in vitro* results, Cyst(e)inase displayed superior efficacy to the standard of care drug fludarabine, exhibiting a significantly longer median survival time of 7 months ($p < 0.0001$). A combination of fludarabine and Cyst(e)inase showed a slight but not statistically significant improvement in median survival ($p = 0.092$, 7.4 months vs. 7 months, Fig. 4b) relative to Cyst(e)inase alone. It is noteworthy that the longest surviving mice in this study were treated with Cyst(e)inase twice a week for over 5 months without any signs of toxicity or weight loss (Supplementary Fig. 10). Finally, we tested the efficacy of Cyst(e)inase, fludarabine, or their combination *ex vivo* against primary leukemia cells isolated from CLL patients with or without 17p deletions, and either cultured alone or co-cultured with the human bone marrow stromal cell line NKTert (as previously stated, co-culture with stromal cells mimics the protective CLL microenvironment). Cyst(e)inase treatment (alone or in combination with fludarabine) was highly efficacious in killing both p17 wt and 17p- CLL cells as assessed by flow cytometry following double staining of cells with Annexin-V and PI (n = 6 CLL patient samples for each phenotype, Fig. 4c,d & Supplementary Fig. 11), even in the presence of stromal cell protection. In contrast, fludarabine treatment alone only moderately impacted p17 wt CLL cells and was far less efficacious against 17p- CLL samples, consistent with the known chemotherapeutic resistance arising from 17p deletions[38]. Both patient-derived CLL cells and mouse *TCL1*-Tg:$p53^{-/-}$ splenocytes showed a marked reduction in GSH levels following treatment with 0.1 μM Cyst(e)inase (Fig. 4e) and a concomitant increase in superoxide levels (Supplementary Fig. 12). Treatment with 0.1 μM Cyst(e)inase had a very slight effect (12% reduction) on the viability of non-malignant B lymphocytes from healthy donors co-cultured with NKTert stromal cells, and even higher concentrations only moderately effected viability (21% and 30% reduction with 0.2 μM or 0.5 μM, respectively, Fig. 4f and Supplementary Fig. 13). In conclusion, Cyst(e)inase was highly effective in treating CLL with 17p deletions, which are more aggressive and resistant to standard of care drugs such as fludarabine[38]. Based on these results we expect that other hematological malignancies with intrinsically high ROS will be impacted by L-Cys and CSSC depletion.

There are several reasons tumors critically depend on the uptake of extracellular L-Cys and CSSC for the production of anti-oxidants. First, inflammation in the tumor microenvironment and the accompanying exogenous ROS stress greatly increase the cellular demand for anti-oxidants[39]. Second, activation of oncogenes such as *c-Myc, Ras* or *Bcr-abl*, loss of functional p53 and metabolic imbalances cause significant increases in internal ROS stress relative to non-malignant tissues[1,40]. Third, many tumors are deficient in expression of transsulfuration pathway enzymes[41], and significant down-regulation of CBS correlates with tumor progression and shorter overall survival[11]. Fourth, there is growing evidence that besides the GSH anti-oxidant pathway, the L-Cys pool in conjunction with the TXN enzymes represents an ancillary redox buffer system[3,42,43] that can compensate for GSH deficiencies.

We show that Cyst(e)inase treatment increases ROS and reduces GSH levels in PCa and CLL models (Fig. 2b,c, Fig. 4e, and Supplementary Fig. 12). In PCa cell lines, the ensuing

increase in ROS mediates the activation of AMPK and the induction of autophagy, consistent with previous observations of the effects of high ROS in tumors[24–26] (Fig. 2d–f and Supplementary Fig. 3b–d). In contrast, CLL cells rapidly undergo apoptosis following Cyst(e)inase treatment (Supplementary Figs. 9 and 11). CLL cells have intrinsically higher basal ROS and lower GSH levels[44], suggesting that they are highly sensitive to additional ROS-mediated damage caused by depletion of L-Cys and CSSC. Likewise, rapid apoptosis is observed in CLL cells treated with the GSH-depleting drug β-phenylethyl isothiocyanate leading to degradation of the anti-apoptotic myeloid cell leukemia 1 protein[44,45] suggesting that there is insufficient time for autophagy to occur in CLL cells.

Collectively our results in conjunction with earlier studies support that cysteine is a critical metabolite for both the GSH and TXN anti-oxidant pathways. As Cyst(e)inase simultaneously affects both GSH and TXN pathways, it is not surprising that it synergizes with other ROS-inducing drugs targeting these pathways such as BSO or curcumin[46,47] (Supplementary Fig. 8). Synergism with curcumin is especially noteworthy because it has been shown to irreversibly inactivate TXNR by covalent modification of two active site residues, in turn inducing NADPH oxidase activity, thus converting the enzyme from an anti-oxidant to a pro-oxidant[34]. Curcumin is currently under evaluation for various neoplasias in at least 8 open clinical trials[35–37]. As many other chemotherapeutic agents are also known to oxidatively stress cancer cells, we expect that Cyst(e)inase will be highly efficacious in combination therapies with other ROS-inducing drugs such as bortezomib or arsenic trioxide[1,48]. Further, by depleting both extracellular CSSC and L-Cys, Cyst(e)inase abrogates the import of L-Cys, a process that is independent of xCT(−) and cannot be targeted by known small molecule drugs.

Online Methods

Protein expression and purification

E.coli-BL21(DE3) cells harboring plasmids of CGL variants were grown in Terrific Broth (TB) media containing 50 μg/mL kanamycin at 37°C to an OD_{600} of ~0.5 at which time Isopropyl β-D-1-thiogalactopyranoside (IPTG; Fisher Scientific) was added to a final concentration of 1 mM. After an additional ~16 hours of incubation at 25°C, cells were collected by centrifugation and re-suspended in immobilized metal affinity chromatography (IMAC) buffer (10 mM $NaPO_4$/ 30 mM imidazole/ 300 mM NaCl, pH 8) additionally containing pyridoxal-5'-phosphate (PLP; 0.5 mM; Sigma), phenylmethanesulfonyl fluoride (PMSF; 10 μM; Sigma), and DNase (1μg/mL; Sigma). The re-suspended cells were then lysed by a French pressure cell, and the lysates were centrifuged at 24,000 × g for 1 hour at 4°C. The resulting supernatant was applied to a nickel IMAC column, washed with 10–20 column volumes of IMAC buffer (containing 0.5 mM PLP), and eluted with 5 column volumes of IMAC elution buffer (50 mM $NaPO_4$/ 250 mM imidazole/ 300 mM NaCl, pH 8). All chromatography was performed at 4°C. Eluted enzyme was then incubated with 10 mM PLP for a minimum of 1 hour at 4°C. Using a 10,000 MWCO centrifugal filter device (Amicon), protein was then buffer exchanged into a solution comprised of phosphate buffered saline (PBS), 10% glycerol, pH 7.4. After sufficient buffer exchange, aliquots of purified enzyme were then flash frozen in liquid nitrogen and stored at −80°C. To determine

protein concentrations, extinction coefficients, were calculated based on amino acid sequence (ε_{280} = 29,870 $M^{-1}cm^{-1}$ for CGL). All protein concentrations were determined from the absorption at 280 nm in 6 M guanidinium hydrochloride, 20 mM phosphate buffer, pH 6.5. Purity of the protein was assessed by SDS-PAGE.

Kinetic assays

Kinetic analyses were performed by measuring pyruvate production from L-Cys or CSSC by reaction with 3-methyl-2-benzothiazolone hydrazone hydrochloride (MBTH; Sigma) to generate a chromophore with a λ_{max} of ~320 nm. Eppendorf tubes (1.5 mL) containing 220 μL of substrate (at various concentrations) or blanks in a 100 mM sodium phosphate buffer, 1 mM EDTA (pH 7.3), and 10 μM PLP were equilibrated in a 37°C heat block for a minimum of five minutes. Reactions were started by adding 20.3 μL of enzyme solution and quenched with 26.7 μL of 50% trichloroacetic acid after a set length of time. All reactions were carried out in triplicate. Reactions and blanks were then mixed with 733 μL of MBTH solution (2.2 mL: 1.6 mL of 1 M sodium acetate buffer pH 5.0 and 0.6 mL of 0.1% MBTH in same) and incubated at 50°C for 40 minutes. After cooling, the samples were transferred to cuvettes and the A_{320} nm was determined. The assay was shown to be linear between 0–250 μM pyruvate with a lower detection limit of ~10 μM. When CSSC was the substrate, additional kinetic analyses were carried out in a continuous assay by detection of free thiol with 5,5'-dithiobis(2-nitrobenzoic acid) (DTNB) using 96-well plates and a microtiter plate reader (Biotek Instruments, Winooski, VT) set at 412 nm.

Diffraction data collection and structure determination

X-ray diffraction data was collected at the Advanced Light source beamline BL 5.0.3 (Berkeley, CA) and processed using the HKL 2000[49] software suite. A significant off-origin peak in the Patterson map (23% of the height of the origin) was observed using the FFT program in the CCP4 suite, implicating the existence of pseudo-translational symmetry (tNCS). The pseudo-translational vector was refined to be (0.5, 0.38, 0.5) using Phaser (CCP4 suite)[50]. Correction of the intensity of this peak allowed for solving the crystal by molecular replacement (MR) with wild type CGL (PDB: 2NMP) as the search model using Phaser[50]. Refinement of the initial model was accomplished through iterative model building in COOT[51] and models were refined using Phenix refine with 5% of the diffraction set as a test for R_{free} cross-validation. Final values of R_{work} and R_{free} were found to be 19% and 23%, respectively. The evaluated CGL-E59T-E339V structure was analyzed using MolProbity, and gave a MolProbity score of 3.18 (73rd percentile), and an all atom clash score of 21.03 (91st percentile). Data collection and refinement statistics are summarized in Supplementary Table 1. Molecular figures were generated using PyMOL[52]. The engineered human cystathionine gamma lyase (E59T, E339V) structure was deposited into the Worldwide Protein Data Bank with the PDB code of 5EIG.

Cell culture

Human prostate cancer (PCa) cell lines LNCaP, DU145 PC3, and 22Rv1 were purchased from the American type culture collection (ATCC; Manassas, VA). Cells were cultured in RPMI-1640 medium (Life Technologies) supplemented with fetal bovine serum (FBS; 10%; Life Technologies). Cell lines were authenticated by genetic biomarkers and mycoplasma

tests were performed by PCR amplification (Applied Biological Materials Inc.) and 4′,6-diamidino-2-phenylindole (DAPI) staining. The murine prostate tumor cell line, HMVP2, was derived from the ventral prostate of one year old HiMyc transgenic mice[23] and cultured in RPMI-1640 medium containing 10% FBS[22]. The human breast cancer cell line MDA-MB-361 (ATCC) was cultured in Dulbecco's modified Eagle medium (DMEM; Lonza) supplemented with 10% FBS and gentamicin (50 μg/mL, Lonza). All cells were cultured at 37°C in 95% air and 5% CO_2.

Isolation of CLL cells and cytotoxicity assays

Primary leukemia cells were isolated from the peripheral blood samples of CLL patients diagnosed according to the NCI criteria[53]. Proper informed consents under a research protocol approved by the Institutional Review Board (IRB) of MD Anderson Cancer Center were obtained from all patients before the collection of blood samples. Primary CLL cells were isolated from blood samples by density gradient centrifugation as described previously[54], and incubated in RPMI-1640 medium supplemented with 10% FBS and Penicillin (100 U/mL) + Streptomycin (100 μg/mL) overnight before testing drug sensitivity by incubation with fludarabine (10 μM; Sigma) or Cyst(e)inase for 48 hours in the presence or absence of human stromal NKTert cells. Mouse splenocytes were isolated from *TCL1*-Tg:*p53*$^{-/-}$ mice, and red blood cells were removed from the splenocytes by ACK lysis buffer (BD Biosciences). After red blood cell lysis, splenocytes were washed with RPMI-1640 culture medium and PBS. On the same day of isolation, the mouse splenocytes were co-cultured with murine stromal KUSA-H cells and treated with fludarabine or Cyst(e)inase for 48 hours. Cell viability and cellular sensitivity to drug treatment *in vitro* was determined by flow cytometry after double staining of 1×10^6 cells with Annexin-V-FITC (BD Biosciences; 556420) and PI (Sigma; P41710) as previously described[55]. All samples were randomly allocated into experimental groups.

Western blotting

The following antibodies were used for western blotting: AMPK (Cell signaling 2532), pAMPK^{Thr172} (Cell signaling 2531), mTOR (Cell signaling 2983), pmTOR^{S2448} (Cell signaling 2971), p70S6K (Cell signaling 9202), pp70S6K^{Thr389} (Cell signaling 9234), S6 Ribo (Cell signaling 2217), pS6 Ribo$^{S235/236}$ (Cell signaling 2211), pS6 Ribo$^{S240/244}$ (Cell signaling 5364), ULK1 (Cell signaling 8054), pULK1^{S555} (Cell signaling 5869), pULK^{S757} (Cell signaling 6888), LC3B (Cell signaling 2775), Cyclin D1 (Cell signaling 2926), cMyc (Cell signaling 5605), CDK2 (Cell signaling 2546), CDK4 (Cell signaling 2906), pRb$^{S807/811}$ (Cell signaling 9308), Cyclin E1 (abcam ab7959), Rb (abcam ab6075), Cyclin A (Santa Cruz sc-596), Cyclin B1(Santa Cruz sc-752), and E2F4 (Santa Cruz sc-866), p27 (BD Biosciences 610242) and β-actin (Sigma-Aldrich A5316). Secondary antibodies were purchased from GE Healthcare.

Cells were treated with indicated concentrations of Cyst(e)inase for the specified time. After incubation, cells were washed with ice-cold PBS and lysed in Radioimmunoprecipitation assay (RIPA) buffer. Proteins were separated by 4–15% SDS-PAGE gel and transferred to a nitrocellulose membrane. After blocking in 5% bovine serum albumin (BSA) for 1 hour, the membranes were probed with specific primary antibodies (listed above) overnight at 4°C.

Following secondary antibody incubation, the membranes were visualized using the commercially available chemiluminescent detection kit (Pierce Biotechnology). Western blots were quantified by densitometry analysis using the freeware ImageJ (National Institutes of Health, Bethesda, MD).

Cynomolgus study

This protocol was approved by the Institutional Animal Care and Use Committee (IACUC) before the initiation of treatment at MPI Research, Inc. Animal welfare for this study was in compliance with the U.S. Department of Agriculture's (USDA) Animal Welfare Act (9 CFR Parts 1, 2 and 3). The Guide for the Care and Use of Laboratory Animals, Institute of Laboratory Animal Resources, National Academy Press, Washington, D.C., was followed. This facility maintains an Animal Welfare Assurance statement with the National Institutes of Health, Office of Laboratory Animal Welfare.

Cyst(e)inase administration and sample collection from cynomolgus monkeys—Two non-naïve male cynomolgus monkeys (age 3 years 2 months – 4 years 2 months at the time of the study initiation) were fasted for 8 hours prior to receiving a single intravenous dose of 8 mg/kg Cyst(e)inase via the saphenous vein. Blood samples of 1.75 mL each were collected pre-dose and at 0.083, 0.25, 1, 3, 6, 24, 48, 72, 96, 120, 168, 216, 264, 336, 408, and 504 hours post-dose via the femoral artery/vein. Samples were acidified with 2% acetic acid and placed on ice following collection and centrifuged at 4°C. The resulting plasma was frozen until analysis.

Analysis of plasma L-Cys and CSSC from cynomolgus monkeys—This assay was designed to measure both unbound L-Cys and CSSC in plasma. Briefly: proteins were precipitated by addition of 3:1 ACN:MeOH to the sample, followed by reduction of CSSC to L-Cys with dithiothreitol (DTT). Free L-Cys was subsequently derivatized with bromobimane, and assayed by LC-MS/MS using a SCIEX API 4000™ mass spectrometer (Applied Biosystems/MDS SCIEX). DL-Cystine-2,2',3,3,3',3'-D6 was used as the internal standard. The Lower Limit of Quantitation (LLOQ) for total L-Cys and CSSC was 0.1 μM. The calibration curve range was 0.1–40 μM.

Humane-care guidelines for mouse studies

Protocols for Cyst(e)inase PK/PD, prostate cancer allograft and xenograft studies, and breast cancer xenograft studies were approved by the Institutional Animal Care and Use Committee of the University of Texas at Austin. All mice were allowed to acclimate for at least 1 week prior to use in experiments. Mice were fed a semi-purified diet (AIN76A, 10 kcal%, Research Diets: PK/PD, HMVP2 allograft and DU145, PC3, and 22Rv1 (PBS control and Cyst(e)inase groups) xenograft studies) or standard irradiated rodent chow (Lab Diet 5053 Irradiated PicoLab Rodent Diet 20; MDA-MB-361 xenograft studies) or a custom diet containing curcumin (Research Diets Inc., New Brunswick, NJ; 22Rv1 xenograft studies (curcumin and Cyst(e)inase/curcumin combo groups)) and water *ad libitum*. For *TCL1*-Tg:$p53^{-/-}$ chronic lymphocytic leukemia mouse studies, all mice were housed under conventional barrier protection in accordance with University of Texas MD Anderson

Cancer Center guidelines, and mouse protocols were approved by the University of Texas MD Anderson Cancer Center Institutional Animal Care Committee.

Cyst(e)inase pharmacodynamics and assessment of serum metabolites from mouse plasma

HPLC grade formic acid, ammonium acetate, and methanol were purchased through Thermo Fisher Scientific (San Jose, CA). DL-Cysteine (2-D, 98%), DL-Cystine (3,3,3',3'-D4, 98%), DL-Glutamic acid (2,4,4-D3, 98%) were purchased from Cambridge Isotope Laboratories (Andover, MA). Mass spectrometry calibration mixtures were also purchased from Thermo Fisher Scientific (Thermo Scientific Pierce LTQ Velos ESI Positive and Negative Ion calibration solutions).

FVB 6–7 week old male mice were injected i.p. with 50 mg/kg body weight of Cyst(e)inase and sacrificed at days 0, 1, 2, 4, & 6 (n = 5 per group) for blood and serum collection. Serum samples were mixed with an internal standard mixture of 10 picomoles each of deuterated cystine, cysteine, & glutamic acid and ultrafiltered[56] using Nanosep Omega centrifugal devices, 3 kDa cutoff (Pall Life Biosciences). The filtered polar fractions were chromatographed using a reverse-phase BEH C18, 1.7 μm, 2.1 × 150 mm column (Thermo Accela 1250 UPLC equipped with a cooling autosampler, Waters Corporation, USA) and introduced into a high-resolution Thermo Scientific Q Exactive Hybrid Quadrupole-Orbitrap mass spectrometer (UHPLC-MS/MS) coupled with electrospray ionization (Thermo Fisher Scientific, San Jose, CA). A gradient elution was used to achieve chromatographic separation with a mobile phase composed of mobile phase A (2 mM $CH_3CO_2NH_4$ with 0.1% formic acid) and mobile phase B (100% methanol). The mobile phase in the gradient elution consisted of 3 steps for a total run time of 10 minutes: 1) a 5 minute gradient of 5% to 95% B; 2) a 2 minute gradient of 95% down to 5% B; and 3) a column re-equilibration with 95% A for 3 minutes. The flow rate was set at 0.3 mL/min. Data acquisition was performed with positive and negative electrospray ionization mode with a spray voltage of 3.5 kV (capillary temperature at 250°C), and was acquired in centroid MS mode from 50 to 700 m/z mass range with the Xcalibur program provided with instrument. Subsequently, the data was exported into MATLAB (Mathworks Inc., MA, USA) and mapped against a database of accurate masses from the KEGG[57], Human Metabolome[58], and Metlin[59] databases. To isolate peaks of interest, a mass tolerance of 3 ppm was applied, and values were reported as ratios normalized to internal standards with the closest chemical features.

Circulatory persistence of Cyst(e)inase

Dot blot analyses with an anti-CGL antibody were used to assess circulatory persistence (PK) of Cyst(e)inase. Samples of either Cyst(e)inase titrations (control) or mouse serum from the aforementioned toxicity study (5 μL appropriately diluted in PBS) were bound to a nitrocellulose membrane positioned in a 96-well dot blot apparatus (Schleicher & Schuell minifold). Membranes were blocked with PBS with 0.05% Tween-20 (PBST) containing 2.5% skim milk powder (PBSTM) for 1 hour at 25°C. The enzyme was then allowed to react with Anti-Cystathionine-γ-lyase isoform 1 antibodies (Sigma; C8248) diluted (1:2000) in PBSTM overnight at 4°C. Following washing with PBST (3× five minute washes), membranes were incubated with a FITC conjugated goat anti-rabbit secondary antibody

(Life Technologies; 65-6111) diluted (1:50) in PBSTM for ~1 hour at 25°C, washed and scanned using the GE Typhoon FLA 9500 imager equipped with a 473 nm laser and an LPB emission filter. Densitometry was performed on scanned dot blots using the freeware ImageJ (National Institutes of Health, Bethesda, MD) and fit as a function of time to calculate half-lives using the software program Kaleidagraph (Reading, PA).

Mouse allograft and xenograft studies

For all allograft and xenograft studies, after the tumors were palpable, mice were randomly divided into treatments groups such that each group had approximately the same starting average tumor size before treatment was initiated. Tumor size was measured 2–3 times weekly using a digital caliper and no blinding during tumor measurement was used. Tumor volume was calculated by the formula: $0.5236\ D1(D2)^2$, where D1 and D2 are the long and short diameter, respectively. Food consumption and body weight of the mice were measured weekly. For all studies dosing was terminated when control tumors reached a maximum tumor volume as pre-specified by a University of Texas Institutional Animal Care and Use Committee (IACUC) approved protocol.

HMVP2 PCa allograft studies—To generate spheroids, HMVP2 cells were plated in ultra-low attaching tissue culture dishes. After 3 days, spheroids were harvested, mixed 1:1 with matrigel (BD Biosciences), and injected subcutaneously into the mouse flank of syngeneic FVB/N male 6–7 week old mice. Treatment was initiated when tumor volume reached 100 mm^3 (day 15) followed by i.p. injections every 4 days with one of the following: PBS (n = 5), heat inactivated Cyst(e)inase (100 mg/kg) (n = 6), 50 mg/kg Cyst(e)inase (n = 7), or 100 mg/kg Cyst(e)inase (n = 7).

DU145 PCa xenograft studies—DU145 cells (2.5×10^6) were mixed with matrigel (1:1) and injected subcutaneously into both flanks of male 6–7 week old athymic nude mice (outbred homozygous nude-*Foxn1*^{nu}/*Foxn1*^{nu}; JAX 007850). Treatment was initiated when tumor volume reached 100 mm^3 (day 9) followed by i.p. injections every 4 days with either PBS or 100 mg/kg Cyst(e)inase (n = 8 per group).

PC3 PCa xenograft studies and analysis of blood and serum toxicity profile—PC3 cells (2.5×10^6) were mixed with matrigel (1:1) and injected subcutaneously into both flanks of male 6–7 week old athymic nude mice (outbred homozygous nude-*Foxn1*^{nu}/*Foxn1*^{nu}; JAX 007850). Treatment was initiated when tumor volume reached 150 mm^3 (day 10) followed by i.p. injections every 4 days with one of the following: PBS, heat inactivated Cyst(e)inase (100 mg/kg), 50 mg/kg Cyst(e)inase, or 100 mg/kg Cyst(e)inase (n = 7 per group).

Following termination of the study, blood was collected by cardiac puncture following euthanasia. Immediately after cardiac puncture, 90 μL of blood was mixed with 10 μL of potassium Ethylenediaminetetraacetic acid (K_2EDTA) solution (18 mg/mL; Fisher Scientific) and red blood cells (RBC) number and size were counted with an automated cell counter (Nexcelom Bioscience). For white blood cells (WBC) the K_2EDTA containing blood was mixed with acridine orange/propidium iodide (1:1) solution (Nexcelom

Bioscience) and number and size of WBC were counted with the same cell counter. Plasma samples were isolated from the remaining blood according to an established procedure[24]. The biochemical parameters of hepatotoxicity: Alanine Aminotransferase (ALT) and Aspartate Aminotransferase (AST); as well as urea level (as an index of renal function) were measured in these samples using commercially available kits (Sigma).

MDA-MB-361 breast cancer xenograft studies—MDA-MB-361 breast cancer cells (1×10^6) were mixed with matrigel (1:1) and injected subcutaneously into the mammary fat pad of female NOD SCID mice (JAX). Treatment was initiated when tumor volume reached 70 mm^3 (day 10) followed by i.p. injections every 3 days with one of the following: PBS (n = 9), 50 mg/kg Cyst(e)inase (n = 10), or 100 mg/kg Cyst(e)inase (n = 9).

22Rv1 CRPC xenograft studies—22Rv1 cells (2×10^6) were mixed with matrigel (1:1) and injected subcutaneously into both flanks of male 6–7 week old athymic nude mice (outbred homozygous nude-*Foxn1*^{nu}/*Foxn1*^{nu}; JAX 007850). Treatment was initiated when tumor volume reached 120 mm^3 (day 8) with one of the following: PBS (ip. injections every 4 days), 25 mg/kg Cyst(e)inase (i.p. injections every 4 days), curcumin (1% w/w in diet fed ad libitum), or combinations of Cyst(e)inase and curcumin (n = 7 per group).

TCL1-Tg:*p53*$^{-/-}$ chronic lymphocytic leukemia mouse studies

Male and female *TCL1*-Tg:*p53*$^{-/-}$ mice at 2 months of age were either untreated (n = 47), or randomly allocated into three survival experimental groups of 10 animals each and treated by i.p. injection with one of the following: fludarabine (34 mg/kg daily for five days followed by three weeks respite until death), Cyst(e)inase (100 mg/kg twice per week until death), or their combination.

Statistical analyses

Data were analyzed using GraphPad Prism software (GraphPad, San Diego, CA) and are presented as mean values ± s.e.m. unless otherwise stated. Statistical analyses were performed using two-sided Student's t-test, one-way ANOVA followed by Tukey's multiple comparison test, or repeated measures two-way ANOVA followed by Bonferroni's multiple comparison test, as applicable. For Kaplan-Meier plots of mouse survival, statistical significance was analyzed by the log-rank (Mantel-Cox) test. Sample variance was not significant between control and treatment groups prior to study onset. Significance was set at $P<0.05$. All statistical tests performed are described in the figure legends. Data are representative of at least three independent experiments unless otherwise indicated. Group sizes for animal experiments were chosen based on prior experience and literature precedence such that sufficient numbers were used to calculate tumor volume means and standard deviations at the endpoints of the experiment. No samples, mice or data points were excluded from the reported analysis.

Supplementary Material

Refer to Web version on PubMed Central for supplementary material.

Acknowledgments

We are grateful to D. Lowe (Aeglea Biotherapeutics), O. Paley, and M. Bonem for assistance with various aspects of this work and data interpretation, and L. Beltran and S. Carbajal for their expert technical assistance. Instrumentation and technical assistance for parts of this work were provided by the Macromolecular Crystallography Facility, with financial support from the College of Natural Sciences, the Office of the Executive Vice President and Provost, and the Institute for Cellular and Molecular Biology at the University of Texas at Austin. Diffraction data was collected at the Advanced Light Source at the Berkeley Center for Structural Biology which is supported in part by the National Institutes of Health, National Institute of General Medical Sciences, and the Howard Hughes Medical Institute. The Advanced Light Source is supported by the Director, Office of Science, Office of Basic Energy Sciences, of the U.S. Department of Energy under Contract No. DE-AC02-05CH11231. This work was supported by funding from: NIH 1 R01 CA172724 (P.H.), NIH 1 R01 CA154754 (G.G., E.S.), NIH 1 RO1CA189623 (E.S., J.D. and G.G.), NCI P30 CA54174 (S. Tiziani.) and Aeglea Biotherapeutics.

References

1. Trachootham D, Alexandre J, Huang P. Targeting cancer cells by ROS-mediated mechanisms: a radical therapeutic approach? Nature Reviews Drug Discovery. 2009; 8:579–591. [PubMed: 19478820]
2. Dixon SJ, Stockwell BR. The role of iron and reactive oxygen species in cell death. Nature chemical biology. 2014; 10:9–17. [PubMed: 24346035]
3. Harris IS, et al. Glutathione and thioredoxin antioxidant pathways synergize to drive cancer initiation and progression. Cancer cell. 2015; 27:211–222. [PubMed: 25620030]
4. Liu H, Zhi Y, Geng G, Yu Z, Xu H. Effect of phenethyl isothiocyanate given at different duration of gestation on the outcome of pregnancy in rats. Journal of hygiene research. 2011; 40:283–286. [PubMed: 21695894]
5. Reliene R, Schiestl RH. Glutathione depletion by buthionine sulfoximine induces DNA deletions in mice. Carcinogenesis. 2006; 27:240–244. [PubMed: 16162646]
6. Belalcázar AD, Ball JG, Frost LM, Valentovic MA, Wilkinson J IV. Transsulfuration Is a Significant Source of Sulfur for Glutathione Production in Human Mammary Epithelial Cells. ISRN Biochem. 2013
7. Persa C, Osmotherly K, Chao-Wei Chen K, Moon S, Lou MF. The distribution of cystathionine β-synthase (CBS) in the eye: implication of the presence of a trans-sulfuration pathway for oxidative stress defense. Experimental eye research. 2006; 83:817–823. [PubMed: 16769053]
8. Vitvitsky V, Thomas M, Ghorpade A, Gendelman HE, Banerjee R. A functional transsulfuration pathway in the brain links to glutathione homeostasis. Journal of Biological Chemistry. 2006; 281:35785–35793. [PubMed: 17005561]
9. You X-J, et al. Expression of cystathionine β-synthase and cystathionine γ-lyase in human pregnant myometrium and their roles in the control of uterine contractility. 2011
10. Zhao H, et al. Frequent Epigenetic Silencing of the Folate-Metabolising Gene Cystathionine-Beta-Synthase in Gastrointestinal Cancer. PloS one. 2012; 7:e49683. [PubMed: 23152928]
11. Kim J, et al. Expression of cystathionine β-synthase is downregulated in hepatocellular carcinoma and associated with poor prognosis. Oncology reports. 2009; 21:1449–1454. [PubMed: 19424622]
12. Timmerman LA, et al. Glutamine Sensitivity Analysis Identifies the xCT Antiporter as a Common Triple-Negative Breast Tumor Therapeutic Target. Cancer cell. 2013
13. Takeuchi S, et al. Increased xCT Expression Correlates With Tumor Invasion and Outcome in Patients With Glioblastomas. Neurosurgery. 2013; 72:33–41.
14. Shiozaki A, et al. xCT, component of cysteine/glutamate transporter, as an independent prognostic factor in human esophageal squamous cell carcinoma. Journal of gastroenterology. 2013:1–11.
15. Doxsee DW, et al. Sulfasalazine-induced cystine starvation: potential use for prostate cancer therapy. The Prostate. 2007; 67:162–171. [PubMed: 17075799]
16. Zhang W, et al. Stromal control of cystine metabolism promotes cancer cell survival in chronic lymphocytic leukaemia. Nature cell biology. 2012; 14:276–286. [PubMed: 22344033]
17. Stone E, et al. De novo engineering of a human cystathionine-gamma-lyase for systemic (L)-Methionine depletion cancer therapy. ACS Chem Biol. 2012; 7:1822–1829. [PubMed: 22963240]

18. Huang S, et al. Site-Directed Mutagenesis on Human Cystathionine-γ-Lyase Reveals Insights into the Modulation of H_2S Production. Journal of molecular biology. 2010; 396:708–718. [PubMed: 19961860]
19. Kumar B, Koul S, Khandrika L, Meacham RB, Koul HK. Oxidative stress is inherent in prostate cancer cells and is required for aggressive phenotype. Cancer research. 2008; 68:1777–1785. [PubMed: 18339858]
20. Afanas'ev I. Reactive oxygen species signaling in cancer: comparison with aging. Aging and disease. 2011; 2:219. [PubMed: 22396874]
21. Höll M, et al. ROS signaling by NADPH oxidase 5 modulates the proliferation and survival of prostate carcinoma cells. Molecular carcinogenesis. 2014
22. Saha A, Blando J, Fernandez I, Kiguchi K, DiGiovanni J. Linneg Sca-1high CD49fhigh prostate cancer cells derived from the Hi-Myc mouse model are tumor-initiating cells with basal-epithelial characteristics and differentiation potential in vitro and in vivo. Oncotarget. 2016
23. Ellwood-Yen K, et al. Myc-driven murine prostate cancer shares molecular features with human prostate tumors. Cancer cell. 2003; 4:223–238. [PubMed: 14522256]
24. Cardaci S, Filomeni G, Ciriolo MR. Redox implications of AMPK-mediated signal transduction beyond energetic clues. Journal of cell science. 2012; 125:2115–2125. [PubMed: 22619229]
25. Ghislat G, Patron M, Rizzuto R, Knecht E. Withdrawal of essential amino acids increases autophagy by a pathway involving Ca2+/calmodulin-dependent kinase kinase-beta (CaMKK-beta). The Journal of biological chemistry. 2012; 287:38625–38636. [PubMed: 23027865]
26. Mungai PT, et al. Hypoxia triggers AMPK activation through reactive oxygen species-mediated activation of calcium release-activated calcium channels. Molecular and cellular biology. 2011; 31:3531–3545. [PubMed: 21670147]
27. Liang J, et al. The energy sensing LKB1–AMPK pathway regulates p27kip1 phosphorylation mediating the decision to enter autophagy or apoptosis. Nature cell biology. 2007; 9:218–224. [PubMed: 17237771]
28. Jones RG, et al. AMP-activated protein kinase induces a p53-dependent metabolic checkpoint. Molecular cell. 2005; 18:283–293. [PubMed: 15866171]
29. Foye, W.; Lemke, T.; Williams, D. Foye's Principles of medicinal chemistry. Lippincott Williams & Wilkins; 2007. 2007
30. West GB, Brown JH. The origin of allometric scaling laws in biology from genomes to ecosystems: towards a quantitative unifying theory of biological structure and organization. Journal of Experimental Biology. 2005; 208:1575–1592. [PubMed: 15855389]
31. Lewerenz J, et al. The Cystine/Glutamate Antiporter System xc− in Health and Disease: From Molecular Mechanisms to Novel Therapeutic Opportunities. Antioxidants & redox signaling. 2013; 18:522–555. [PubMed: 22667998]
32. Kato S, Ishita S, Sugawara K, Mawatari K. Cystine/glutamate antiporter expression in retinal müller glial cells: Implications for DL-alpha-aminoadipate toxicity. Neuroscience. 1993; 57:473–482. [PubMed: 7906874]
33. Narang VS, Pauletti GM, Gout PW, Buckley DJ, Buckley AR. Suppression of cystine uptake by sulfasalazine inhibits proliferation of human mammary carcinoma cells. Anticancer research. 2002; 23:4571–4579.
34. Fang J, Lu J, Holmgren A. Thioredoxin reductase is irreversibly modified by curcumin a novel molecular mechanism for its anticancer activity. Journal of Biological Chemistry. 2005; 280:25284–25290. [PubMed: 15879598]
35. Kanai M, et al. A phase I study investigating the safety and pharmacokinetics of highly bioavailable curcumin (Theracurmin®) in cancer patients. Cancer chemotherapy and pharmacology. 2013; 71:1521–1530. [PubMed: 23543271]
36. Carroll RE, et al. Phase IIa clinical trial of curcumin for the prevention of colorectal neoplasia. Cancer Prevention Research. 2011; 4:354–364. [PubMed: 21372035]
37. Kanai M, et al. A phase I/II study of gemcitabine-based chemotherapy plus curcumin for patients with gemcitabine-resistant pancreatic cancer. Cancer chemotherapy and pharmacology. 2011; 68:157–164. [PubMed: 20859741]

38. Liu J, et al. Loss of p53 and altered miR15-a/16-1→ MCL-1 pathway in CLL: insights from TCL1-Tg: p53−/− mouse model and primary human leukemia cells. Leukemia. 2014; 28:118–128. [PubMed: 23608884]
39. Olsen LF, Issinger O-G, Guerra B. The Yin and Yang of redox regulation. Redox Report. 2013; 18:245–252. [PubMed: 24112960]
40. Vousden KH, Ryan KM. p53 and metabolism. Nature Reviews Cancer. 2009; 9:691–700. [PubMed: 19759539]
41. Zhang W, et al. Expression profiling of homocysteine junction enzymes in the NCI60 panel of human cancer cell lines. Cancer research. 2005; 65:1554–1560. [PubMed: 15735045]
42. Mandal PK, et al. System xc− and thioredoxin reductase 1 cooperatively rescue glutathione deficiency. Journal of Biological Chemistry. 2010; 285:22244–22253. [PubMed: 20463017]
43. Pader I, et al. Thioredoxin-related protein of 14 kDa is an efficient L-cystine reductase and S-denitrosylase. Proceedings of the National Academy of Sciences. 2014; 111:6964–6969.
44. Trachootham D, et al. Effective elimination of fludarabine-resistant CLL cells by PEITC through a redox-mediated mechanism. Blood. 2008; 112:1912–1922. [PubMed: 18574029]
45. Zhang W, et al. Effective elimination of chronic lymphocytic leukemia cells in the stromal microenvironment by a novel drug combination strategy using redox-mediated mechanisms. Molecular medicine reports. 2015; 12:7374–7388. [PubMed: 26458979]
46. Lee W-J, et al. Nonautophagic cytoplasmic vacuolation death induction in human PC-3M prostate cancer by curcumin through reactive oxygen species-mediated endoplasmic reticulum stress. Scientific reports. 2015; 5:10420. [PubMed: 26013662]
47. Sánchez Y, Simón GP, Calviño E, de Blas E, Aller P. Curcumin stimulates reactive oxygen species production and potentiates apoptosis induction by the antitumor drugs arsenic trioxide and lonidamine in human myeloid leukemia cell lines. Journal of Pharmacology and Experimental Therapeutics. 2010; 335:114–123. [PubMed: 20605902]
48. Chaiswing L, Zhong W, Liang Y, Jones DP, Oberley TD. Regulation of prostate cancer cell invasion by modulation of extra-and intracellular redox balance. Free Radical Biology and Medicine. 2012; 52:452–461. [PubMed: 22120495]

Online Methods References

49. Minor, W.; Otwinowski, Z. Methods in Enzymology, Macromolecular Crystallography. New York: Academic Press; 1997. HKL2000 (Denzo-SMN) Software Package. Processing of X-ray Diffraction Data Collected in Oscillation Mode.
50. McCoy AJ, et al. Phaser crystallographic software. J Appl Crystallogr. 2007; 40:658–674. [PubMed: 19461840]
51. Emsley P, Lohkamp B, Scott WG, Cowtan K. Features and development of Coot. Acta Crystallogr D Biol Crystallogr. 2010; 66:486–501. [PubMed: 20383002]
52. DeLano WL. The PyMOL molecular graphics system. 2002
53. Cheson BD, et al. Guidelines for clinical protocols for chronic lymphocytic leukemia: Recommendations of the national cancer institute-sponsored working group. American journal of hematology. 1988; 29:152–163. [PubMed: 3189311]
54. Huang P, Sandoval A, Van Den Neste E, Keating M, Plunkett W. Inhibition of RNA transcription: a biochemical mechanism of action against chronic lymphocytic leukemia cells by fludarabine. Leukemia (08876924). 2000; 14
55. Pelicano H, et al. Inhibition of mitochondrial respiration a novel strategy to enhance drug-induced apoptosis in human leukemia cells by a reactive oxygen species-mediated mechanism. Journal of Biological Chemistry. 2003; 278:37832–37839. [PubMed: 12853461]
56. Tiziani S, et al. Optimized metabolite extraction from blood serum for H-1 nuclear magnetic resonance spectroscopy. Anal. Biochem. 2008; 377:16–23. [PubMed: 18312846]
57. Okuda S, et al. KEGG Atlas mapping for global analysis of metabolic pathways. Nucleic Acids Research. 2008; 36:W423–W426. [PubMed: 18477636]
58. Wishart DS, et al. HMDB: the human metabolome database. Nucleic Acids Research. 2007; 35:D521–D526. [PubMed: 17202168]

59. Sana TR, Roark JC, Li X, Waddell K, Fischer SM. Molecular formula and METLIN Personal Metabolite Database matching applied to the identification of compounds generated by LC/TOF-MS. Journal of biomolecular techniques: JBT. 2008; 19:258. [PubMed: 19137116]

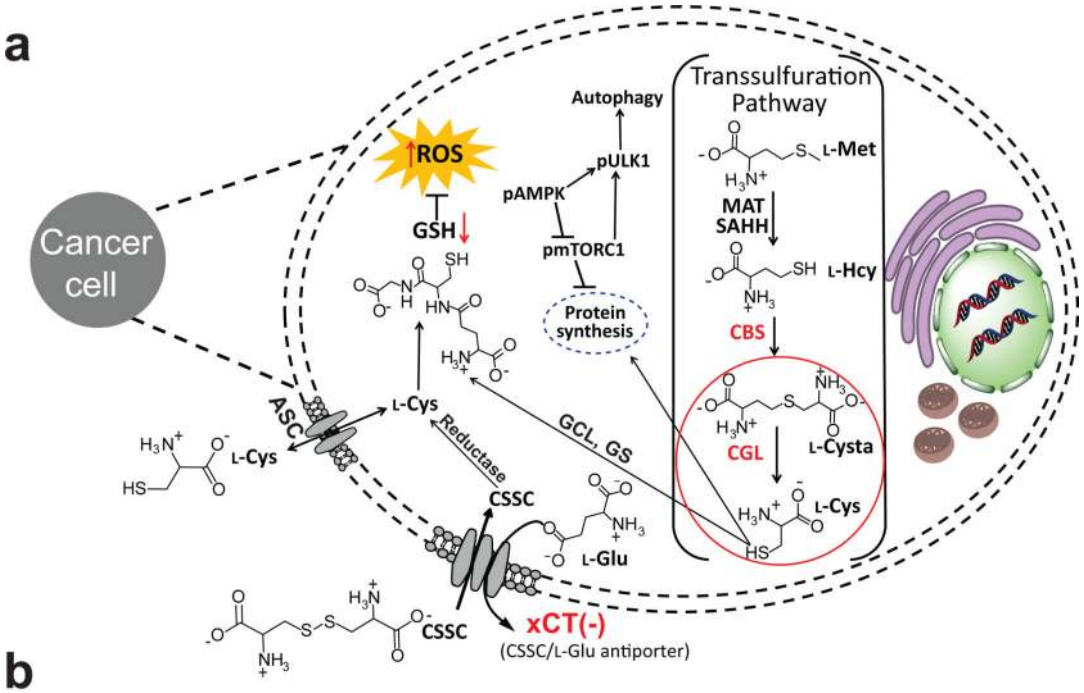

b

Substrate	Human cystathionine-γ-lyase (CGL)			Engineered Cyst(e)inase		
	$k_{cat}(s^{-1})$	$K_M(mM)$	$k_{cat}/K_M(mM^{-1}s^{-1})$	$k_{cat}(s^{-1})$	$K_M(mM)$	$k_{cat}/K_M(mM^{-1}s^{-1})$
CSSC	0.23 ± 0.03	0.27 ± 0.07	0.85 ± 0.25	2.6 ± 0.1	0.06 ± 0.01	43 ± 7 (50)
L-Cys	0.15 ± 0.02	0.79 ± 0.30	0.20 ± 0.10	1.7 ± 0.05	0.33 ± 0.03	5.1 ± 0.5 (25.5)
L-Cysta	3.7 ± 0.2	0.40 ± 0.07	9.3 ± 1.7	1.0 ± 0.03	1.9 ± 0.2	0.53 ± 0.05 (0.06)

() = fold change from CGL

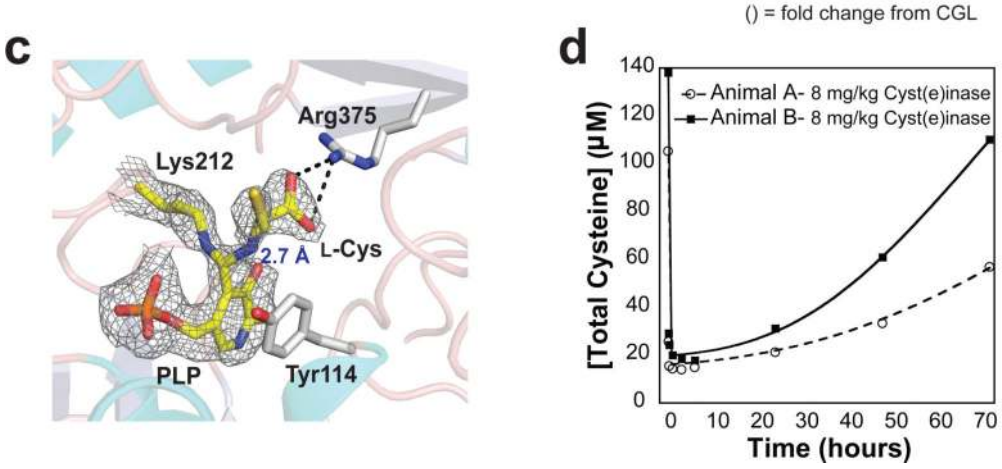

Figure 1. Engineered human Cyst(e)inase for cancer treatment

(**a**) Schematic of the therapeutic effect of Cyst(e)inase treatment on cancer cells. Mutations in the transsulfuration pathway and/or elevated ROS production in cancer outstrips the normal L-Cys production capacity needed for GSH and protein synthesis, causing tumors to rely instead upon L-Cys import predominantly via the xCT(−) antiporter mediated exchange of L-Glu for extracellular CSSC. Therapeutic depletion of extracellular L-Cys and CSSC selectively targets cancers cells causing potent growth arrest and killing, increased levels of ROS, decreased levels of GSH, and induction of autophagy. (Abbr. L-Met = L-methionine, L-

Hcy = L-homocysteine, MAT = methionine adenosyl transferase, SAHH = S-adenosylhomocysteine hydrolase, GCL = glutamate-cysteine ligase, GS = glutathione synthase). (**b**) Michaelis-Menten parameters for Cyst(e)inase and CGL. Results are from experiments performed in triplicate, data is expressed as mean ± s.d. (**c**) Structural analysis of Cyst(e)inase reveals the formation of a geminal diamine reaction intermediate with substrate L-Cys. (**d**) Time course of total serum Cysteine (free L-Cys + reduced CSSC + liberated protein-bound L-Cys) following single dose administration of Cyst(e)inase at 8 mg/kg in two cynomolgus monkeys.

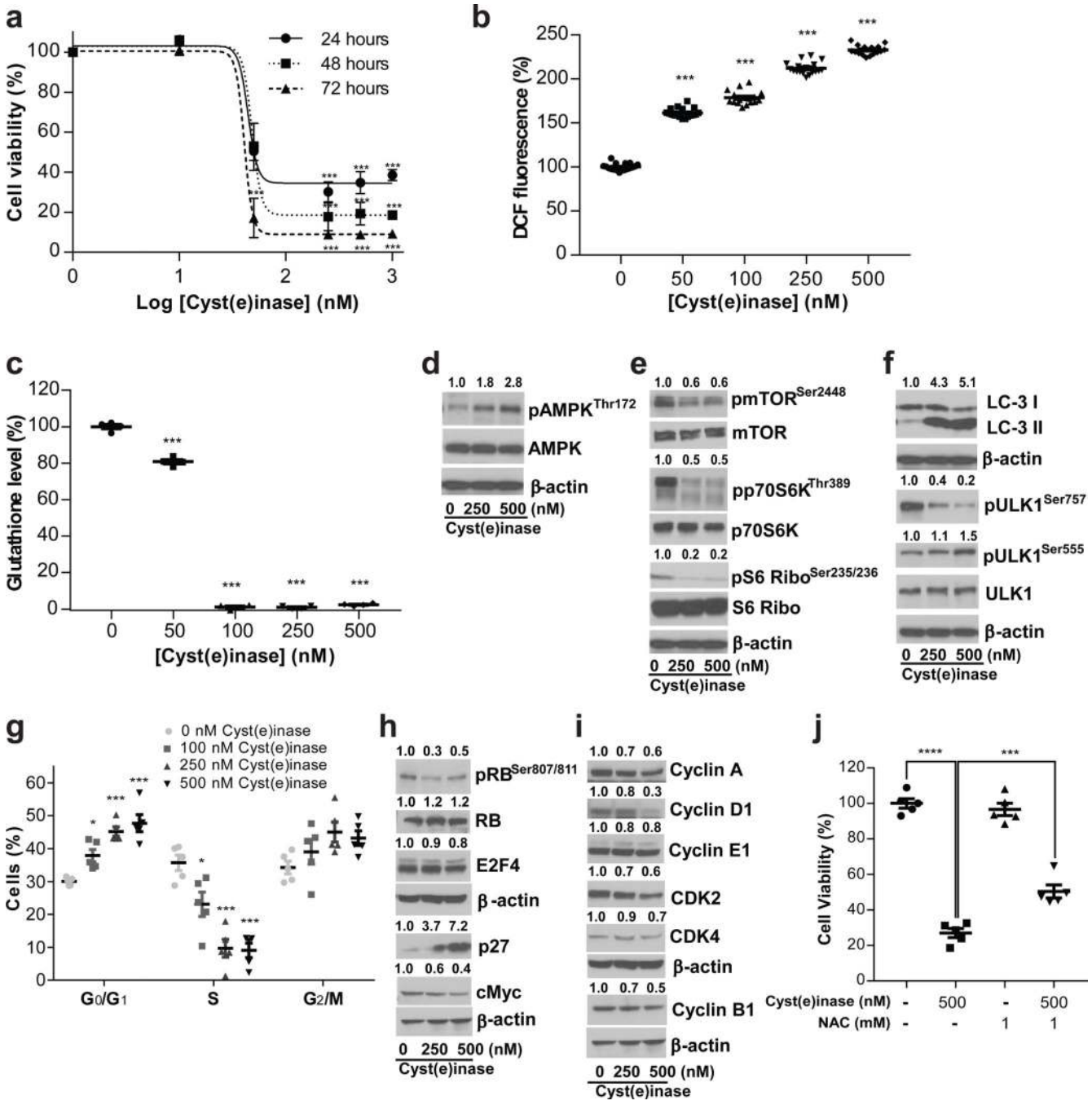

Figure 2. Effect of Cyst(e)inase in PCa cells

(a–c) HMVP2 cells were treated with indicated concentrations of Cyst(e)inase. (**a**) Cell viability as assessed by alamar blue assay at indicated time points. (**b**) Relative cellular ROS levels 4 h post-treatment as assessed by 2′,7′-Dichlorofluorescin diacetate (DCFDA) fluorescence; (**c**) Relative GSH levels 24 h post-treatment as assessed by spectrophotometric analysis. (**d–i**) HMVP2 cells were treated with indicated concentrations of Cyst(e)inase for 24 hours. (**d,e,f,h,i**) Metabolic stress markers and regulatory cell cycle proteins were measured by immunoblot. Immunoblots were performed at least three times with β-actin

controls for each experiment. Numbers above blots indicate band intensities relative to untreated conditions. Images have been cropped for presentation, uncropped images are shown in Supplementary Fig. 14. (**g**) Cell-cycle phase distribution was analyzed by Guava-based flow cytometry 24 h post treatment. (**j**) DU145 PCa cells were treated with indicated concentrations of Cyst(e)inase and/or N-Acetyl-L-Cysteine (NAC) for 48 h and cell viability was assessed by crystal violet assay. For (**a–c, g, j**): data are expressed as mean ± s.e.m; *P<0.05; ***P<0.001; ****P<0.0001; one-way ANOVA followed by Tukey's multiple comparison test (**a–c, g**) or Bonferroni's multiple comparison test (**j**).

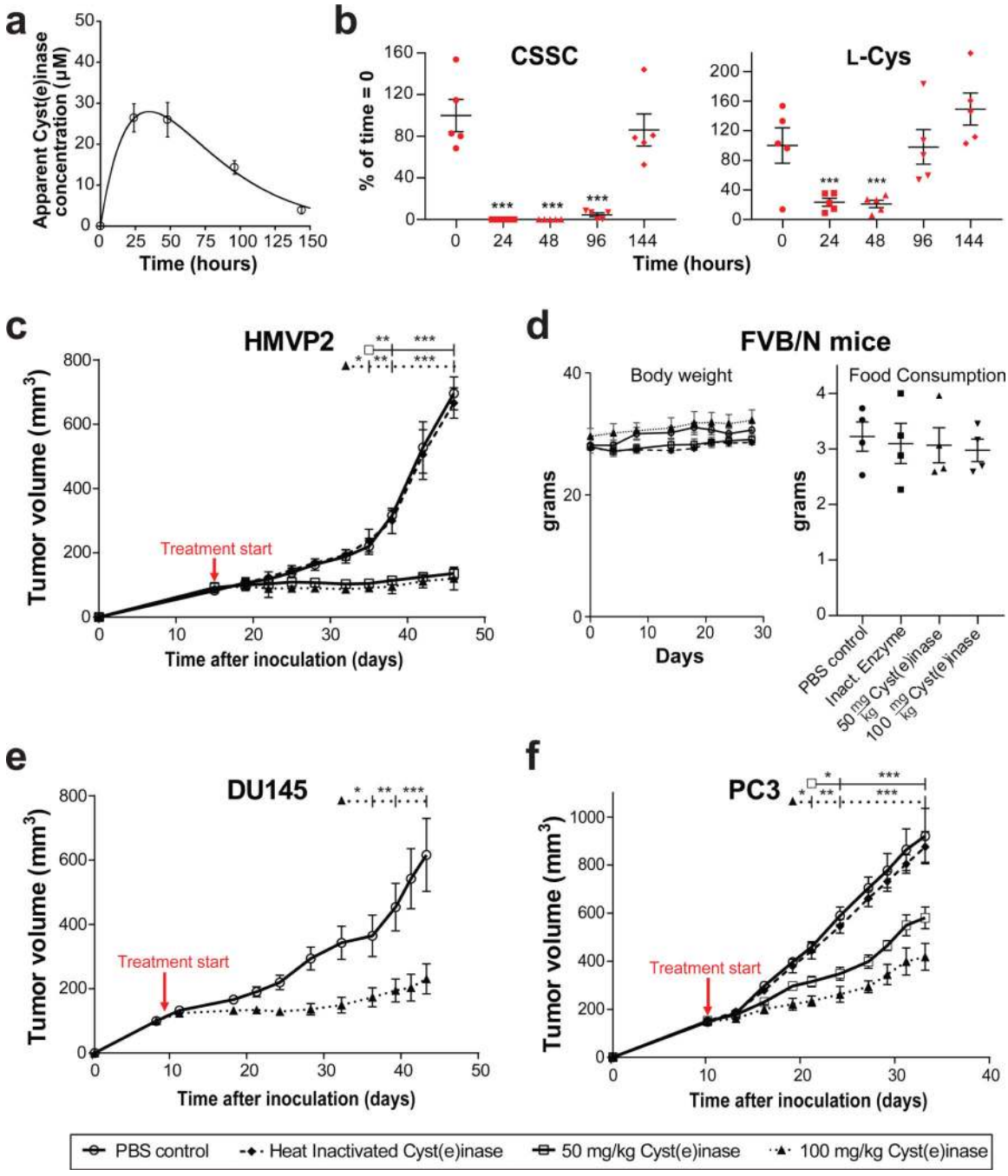

Figure 3. Pharmacokinetics, pharmacodynamics and efficacy of Cyst(e)inase administration in mice

(**a,b**) Following single dose Cyst(e)inase administration at 50 mg/kg in FVB mice, (**a**) apparent Cyst(e)inase concentration in serum as measured by dot blot assay; and (**b**) relative concentrations of L-Cys and CSSC as assessed by MS as a function of time (n = 5 per group). * P<0.05; ** P<0.01; *** P<0.001; two-sided Student's t-test. (**c–d**) Following treatment with active Cyst(e)inase or controls in male FVB/N mice bearing allograft tumors of HMVP2 PCa spheroids; (**c**) quantification of tumor volume; and (**d**) average body weight

and food consumption per mouse per day for each treatment group. (PBS, n = 5; heat inactivated Cyst(e)inase, n = 6; 50 mg/kg Cyst(e)inase, n = 7; 100 mg/kg Cyst(e)inase, n = 7). (**e–f**) Following treatment with active Cyst(e)inase or controls, quantification of tumor volume in male nude mice bearing xenograft tumors of (**e**) DU145 PCa cells (n = 8 per group); and (**f**) PC3 PCa cells (n = 7 per group). For all studies dosing was terminated when control tumors reached an endpoint. For **c, e, f** *P<0.05; **P<0.001; *** P<0.0001; repeated measures two-way ANOVA followed by Bonferroni's multiple comparison test; all data are expressed as mean ± s.e.m.

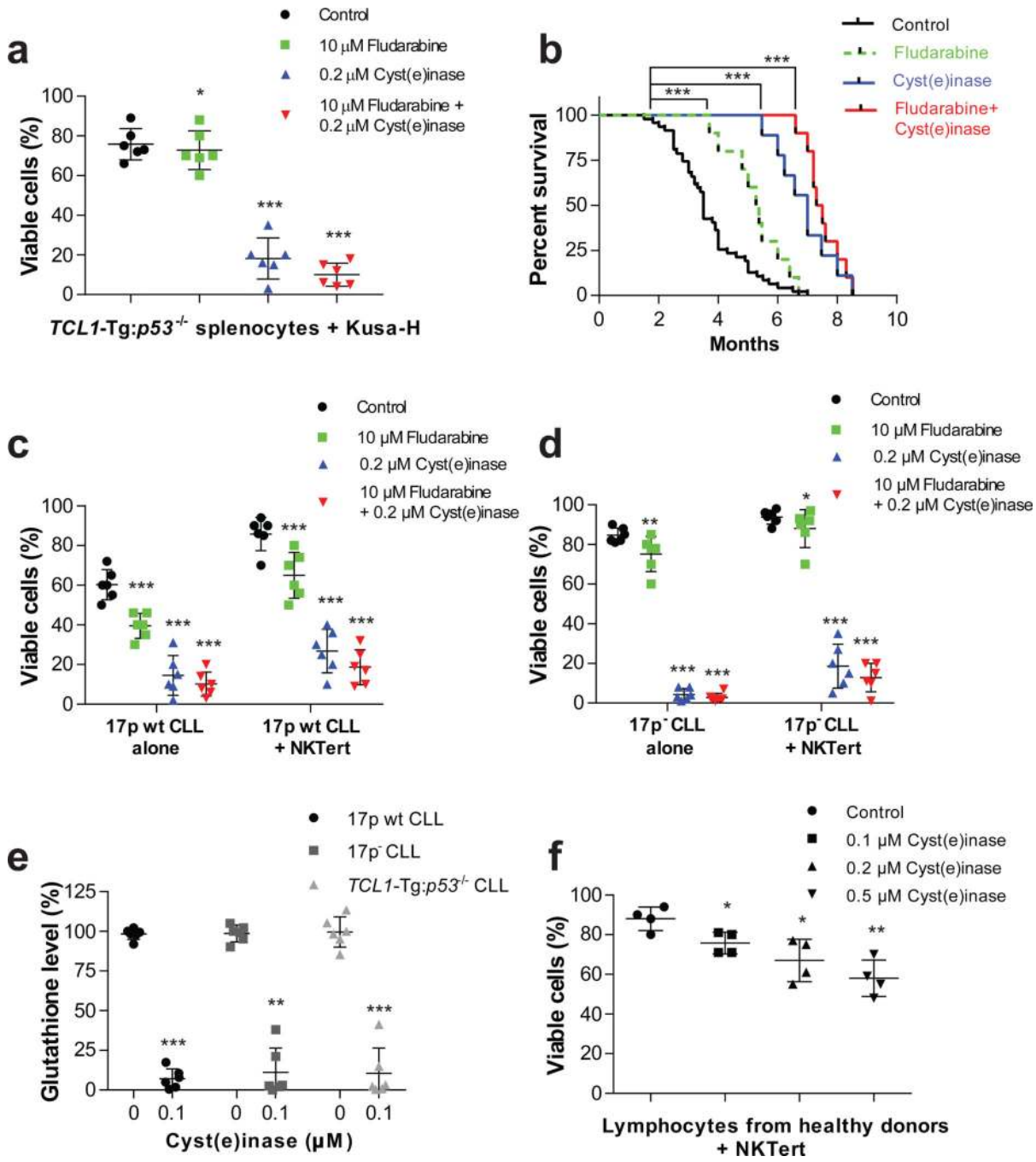

Figure 4. *In vitro* and *in vivo* efficacy of Cyst(e)inase in the *TCL1*-Tg:*p53*$^{-/-}$ mouse model and primary CLL cells

(a) Cell viability 48 h after treatment with fludarabine, Cyst(e)inase, or their combination in splenocytes isolated from *TCL1*-Tg:*p53*$^{-/-}$ mice co-cultured with murine stromal Kusa-H cells (n = 6 per group). **(b)** Survival curve (Kaplan-Meier) of *TCL1*-Tg:*p53*–/– mice following either no treatment (n = 47); or treatment with fludarabine (n = 10); Cyst(e)inase (n=10); or their combination (n = 10). **(c–d)** Cell viability 48 h after treatment with fludarabine, Cyst(e)inase, or their combination in (c) primary 17p wt CLL cells; and (**d**)

primary 17p- CLL cells either cultured alone or co-cultured with stromal NKTert cells (n = 6 different CLL patient samples per phenotype). **(e)** Relative GSH levels as assessed by spectrophotometric analysis 24 h after treatment with Cyst(e)inase in primary 17p wt, 17pCLL cells, and mouse splenocytes isolated from *TCL1*-Tg:$p53^{-/-}$ mice (n = 6 per group). **(f)** Cell viability 48 h after treatment with Cyst(e)inase in normal lymphocytes isolated from healthy donors co-cultured with NKTert cells (n = 4). For (**a, c, d, f**) cell viability was assessed by flow cytometry following double staining of cells with Annexin-V and PI. Data are expressed as mean ± s.d. (**a, c–f**). *P<0.05; **P<0.01; ***P<0.001; two-sided Student's t-test (**a, c–f**) or log-rank (Mantel-Cox) test (**b**).